MICROTREMORS, A NEAR-SURFACE PHENOMENON?

D. NIETO[1], L. BARADELLO[1], S.I. KAKA[2] and A. VESNAVER[1,2]

[1] *Italian National Institute of Oceanography and Applied Geophysics, Trieste, Italy.*
[2] *King Fahd University of Petroleum and Minerals, Dhahran, Saudi Arabia.*
vesnaver@kfupm.edu.sa

(Received October 2, 2011; revised version accepted October 24, 2011)

ABSTRACT

Nieto, D., Baradello, L., Kaka, S.I. and Vesnaver, A., 2011. Microtremors, a near-surface phenomenon? *Journal of Seismic Exploration*, 20: 379-398.

Microtremor measurements have been used for shallow engineering investigations for decades, but recently have been proposed as possible direct hydrocarbon indicators. In this paper, we have carried out field experiments to analyze some microtremors' features as average polarization and statistical stability. Our results seem to confirm the shallow nature of most microtremors' energy, although well data is still needed for a conclusive assessment.

KEY WORDS: microtremor, near-surface, polarization, repeatability, passive seismic.

INTRODUCTION

The dominant energy share of surface waves with respect to body waves (i.e., P- and S-waves) is well known to geophysicists and presents huge challenges in processing active land seismic data to reduce Rayleigh waves or, in jargon, the ground roll. A theoretical study was carried by Miller and Pursey (1955) for a circular source vibrating over a semi-infinite half-space. They proved that about 67% of the elastic energy released at the earth's surface is converted into ground roll, i.e., a much larger share than S-waves (26%) and P-waves (7% only). Similarly, we do not expect major differences with respect to both artificial and natural sources, such as ocean waves impinging the coasts, wind shaking the trees, or simply noise from factory and machineries or vehicles travelling on highways.

0963-0651/11/$5.00 © 2011 Geophysical Press Ltd.

A further factor that enhances the surface waves' energy is the geometric spreading of surface waves with respect to the body waves: cylindrical versus spherical, for a propagation over a simple homogeneous half-space. The real earth's response is more complex, but the amplitude decay of body waves remains faster than that of surface waves.

Early applications of microtremors date back to Nakamura (1989) and Lermo and Chavez-Garcia (1993), among others. They used microtremors to predict the ground response to major earthquakes at specific sites, so highlighting their very local and shallow information. Okada (2003) developed a method for shallow engineering investigations using microtremors, particularly in urban or environmentally sensitive areas where conventional techniques are precluded. He used arrays of vertical-component receivers to recognize and filter the different wave types recorded by the network. For further details on the method and a literature review, we refer the reader to Bonnefoy-Claudet et al. (2006). They suggest using "microtremors" for the ambient wavefield above 1 Hz only, and hence our primary interest in this paper lies in microtremors. Nevertheless, Ruigrok et al. (2011a, b) were able to detect a large portion of body waves in the ambient noise in the frequency band of 0.4-1 Hz.

Microtremors have been recorded worldwide in many different conditions (Aki and Richards, 1980; Peterson, 1993), but the trend of their frequency spectra is quite similar. A general agreement exists in relating very low frequencies (1 Hz and less) to ocean waves impinging the coasts and propagating for very long distances across all continents (see, e.g., Gerstoft et al., 2006; Zhang et al., 2009). Their propagation path include both surface waves as well as diving or head body waves; the latter ones may have an incidence angle close to the vertical. In addition, cultural noise generated by human activities is generally observed in frequencies above 1 Hz or so. However, observation of intermediate frequency range between 2 and 6 Hz is currently being debated (Lambert et al., 2009a, 2010a; Green and Greenhalgh, 2009, 2010), and in this paper we attempt to contribute to this debate by providing new experimental data.

Lambert et al. (2009a, b) reported an empirical correlation between spectral anomalies between 2 and 3 Hz and the underlying presence of hydrocarbons at an oil field in Austria, and comparable experiments were conducted by Saenger et al. (2009) in Mexico and Riahi et al. (2011) in Wyoming (USA). A similar correlation was found by van Maastrigt and Al-Dulaijan (2008) in the Rub-al-Khali desert in Saudi Arabia. These latter ones proposed a possible explanation for this phenomenon by assuming that the dominant propagation of seismic waves is vertical; passing through the hydrocarbon reservoir, the microtremor wavefield is "filtered" and retains the reservoir footprint in this frequency range up to the Earth surface. Supporting

theories were presented by Frehner et al. (2009) and Holzner et al. (2009), but when rock parameters from real carbonate reservoirs are used (Broadhead, 2010), these theories predict spectral anomalies at over 20 Hz instead. Therefore, none of the theoretical models proposed so far can fully explain the experiments reported above.

Berteussen et al. (2008) and Ali et al. (2010) presented experimental results over the boundaries of a producing oil field in the United Arab Emirates. They found remarkable correlations of microtremors with hurricanes and human activities, but none with the underlying reservoir. They also found the dominant direction of microtremors wave pointing towards the coasts of the Arabian Gulf, thus supporting a near-surface origin for the observed wavefield. Similar conclusion was drawn by Hanssen and Bussat (2008) for a profile in the Libyan desert. Although they observed occasional correlation between low-frequency spectral anomalies and the hydrocarbon reservoir, the most striking correlation, however, was found between these anomalies and the sand dunes' topography.

The explanation of these phenomena is still an open problem (Green and Greenhalgh, 2009). New processing techniques have been proposed, as reverse-time imaging (Witten and Artman, 2011) and a correlation analysis with reservoir attributes (Riahi et al., 2011). However, we believe that any solid physical experiment must be repeatable in time, if it represents a quasi-static property as the hydrocarbon saturation of a reservoir. For this reason, we acquired new microtremors data to study its origin and quantify its stability and found interesting new clues using the polarization analysis.

EXPERIMENTAL DESIGN

The measurement of seismic waves with frequencies between 2 and 6 Hz is optimal when using geophones with a peak frequency within that range. A few three-component receivers of that type were available, i.e., 4.5-Hz model TDC-1 (Mark Products), but a much larger number of 10-Hz ones was available too (model GS-30CT, Geo Space). The latter ones are much cheaper and hence their use might allow future large-scale surveys. Also, bulky and expensive 1-Hz vertical-component receivers model L-4 (Mark Products) are appropriate for the frequency range that we are interested in. We planted them very close to one another (Fig. 1) and recorded the microtremor signal for the period of 10 minutes, with a sampling rate of 1 millisecond. Fig. 2 displays the resulting amplitude spectra of the vertical component in the frequency interval from 0 to 10 Hz at a semi-logarithmic scale. The main differences are visible on the right, between 8 and 10 Hz, while they are much lower in the band of interest (2-6 Hz).

All three *amplitude* spectra show large values in the frequencies below 2 Hz, as observed in most other parts of the world (Peterson 1993, Okada 2003).

Fig. 1. The sensors we compared with different frequency peak: 1 Hz (left, grey, vertical component only), 4.5 Hz (right, orange, three-component) and 10 Hz (yellow, in the back, three-component).

At a first glance, their trend resembles the so-called "pink" or "1/f" noise, whose *power* spectrum is inversely proportional to the frequency. This type of noise occurs in electronic equipments, and its level is related to the Brownian motion of electrons. Furthermore, it occurs in several natural phenomena in a quasi-equilibrium state, including meteorological (Selvam and Fadnavis, 1998; Fraedrich and Blender, 2003; Fraedrich et al., 2004) and geophysical phenomena (Mandelbrot and Wallis, 1969; Holliger, 1996; Telesca et al., 2002; Davidsen and Schuster, 2002). Modern recording equipments are manufactured to minimize such a distortion source, and in the Appendix we quantify the possible instrumental contribution with respect to the signal level in our specific case.

If the signal spectrum S(f) may be approximated by an inverse function of the frequency f:

$$S(f) \propto K/f \quad , \tag{1}$$

where K is a constant, then multiplying each side by f we get:

$$S(f)f \propto K \quad . \tag{2}$$

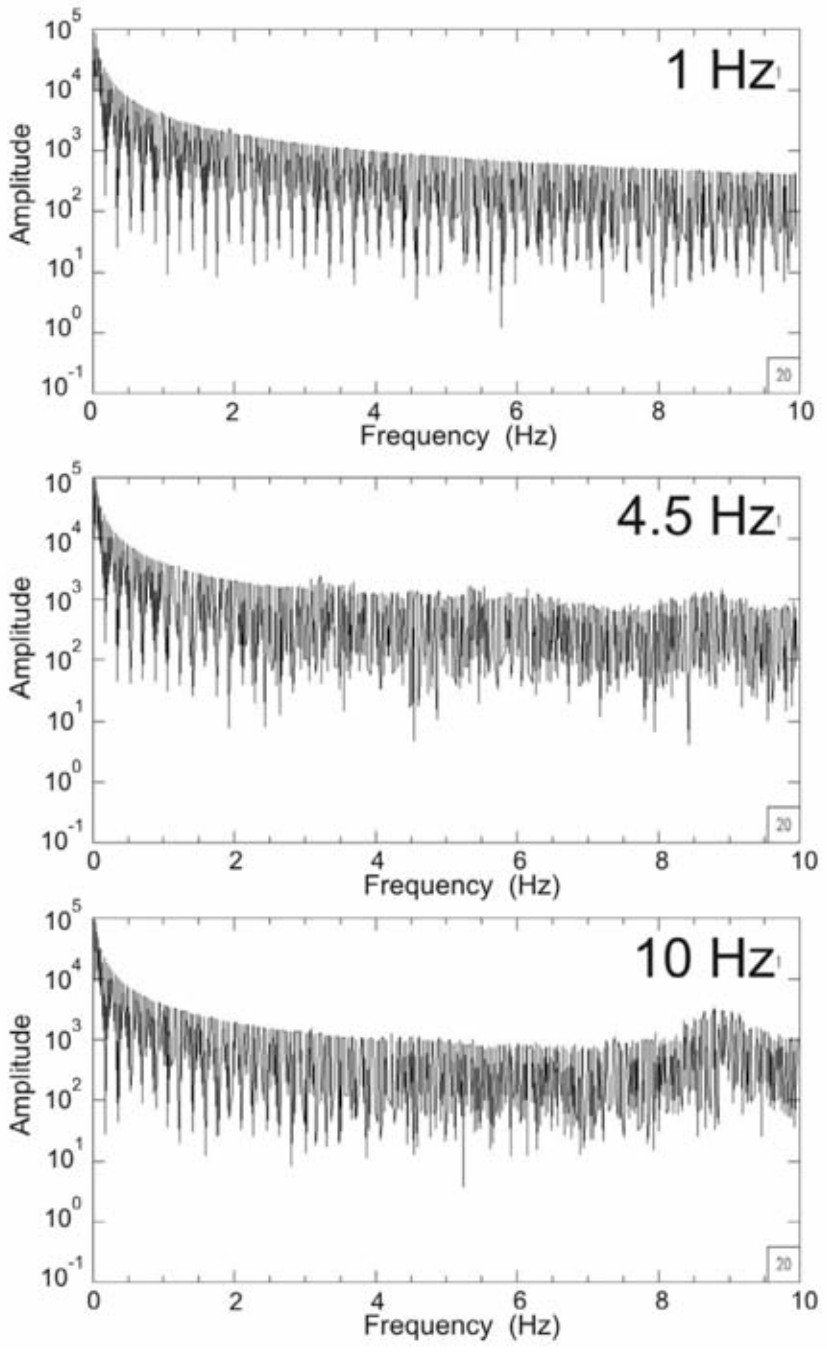

Fig. 2. Comparison of the frequency spectra obtained from simultaneous records of the three geophones in Fig. 1, for a duration of 10 minutes. The horizontal scale is linear, while the vertical one is logarithmic. The differences in the band of interest (2-6 Hz) are modest.

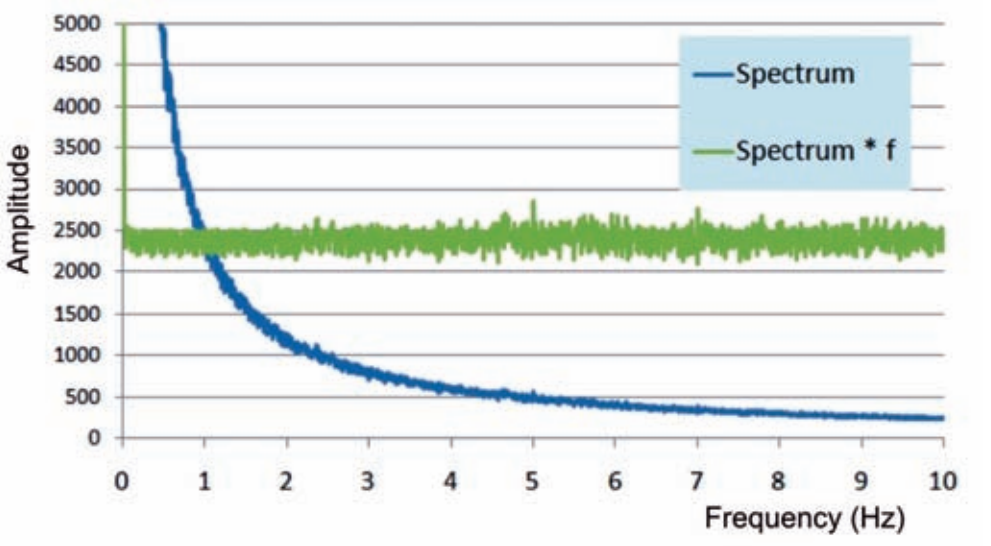

Fig. 3. Comparison at a linear scale between an averaged spectrum of the 1Hz receiver (blue line) and its corresponding value multiplied by the frequency (green line).

Fig. 3 displays at a linear scale the amplitude spectrum from a 1-Hz receiver, smoothed by averaging 10 adjacent frequency values, and such a smoothed spectrum multiplied by the frequency f. The resulting latter function is quite flat, so meaning that the recorded ambient noise has such a power spectral trend as $1/f^2$. Such a type is call "red" or "Brown" noise, and it is clearly different from the possible instrumental noise contribution.

Fig. 4 allows comparing further the response of the different receivers in the range we are interested in, i.e., between 2 and 6 Hz. For improving the statistical stability in time, we divided the 10-minutes records into chunks of 30 s each and computed the amplitude spectra for each chunk, taking their average. We see in the figure that the spectra are not so similar, but all display comparable energy in the range between 3 and 7 Hz. Thus, although the 4.5-Hz receiver is the most appropriate, the much cheaper 10-Hz one is an acceptable replacement for our purposes. A large number of these receivers allow us building 2D arrays in our future experiments.

A key decision to be taken to study an ubiquitous phenomenon as microtremors is the optimal location. Optimal does not necessarily mean perfectly quiet, because the practical use of extreme, unusual cases is minimum.

Thus, we compared the data from three different locations in North-Eastern Italy: a very noisy one as the parking lot of OGS headquarters, an intermediate one at the OGS test site for geophysical data acquisition in Torrate, and the very quiet one in the Giant Cave near Trieste. Three-component receivers were used to be able to analyze the wave polarization.

Fig. 5 displays the particle motion plot in the three cases, with the three projections in the vertical and horizontal planes. The duration of the records in this and following figures is 10 minutes. As expected, the plots for the parking lot do not show any preferential direction, because the noise sources (mainly cars and walking people) change very often. The interpretation of the strong polarization in the quiet case (Giant Cave), and even less in the intermediate one, is not so obvious. The latter one is located in Torrate, a rural area relatively far from factories and major highways, where fresh water is produced because of shallow aquifers; nonetheless, it is not too quiet either, because occasionally cars pass through a local road nearby and some water pumps are activated at irregular time intervals. In other words, this site is representative for the normal conditions of possible land data acquisitions in Europe and similar areas worldwide. For this reason, we continued the data collection in this area, as it displays both this interesting polarization feature and the challenge of a realistic environmental noise.

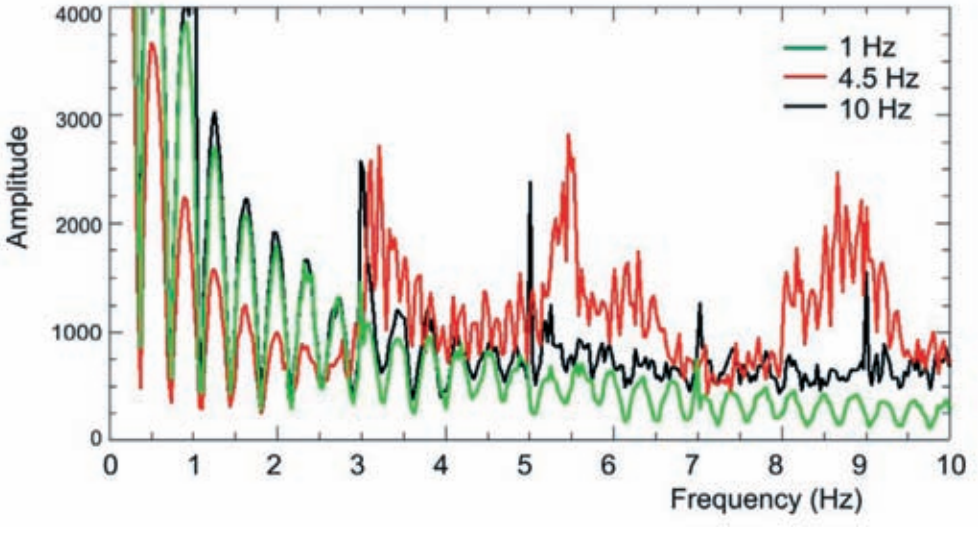

Fig. 4. Comparison at a linear scale between the spectra obtained from the different receivers: 1 Hz (green line), 4.5 Hz (red line) and 10 Hz (black line).

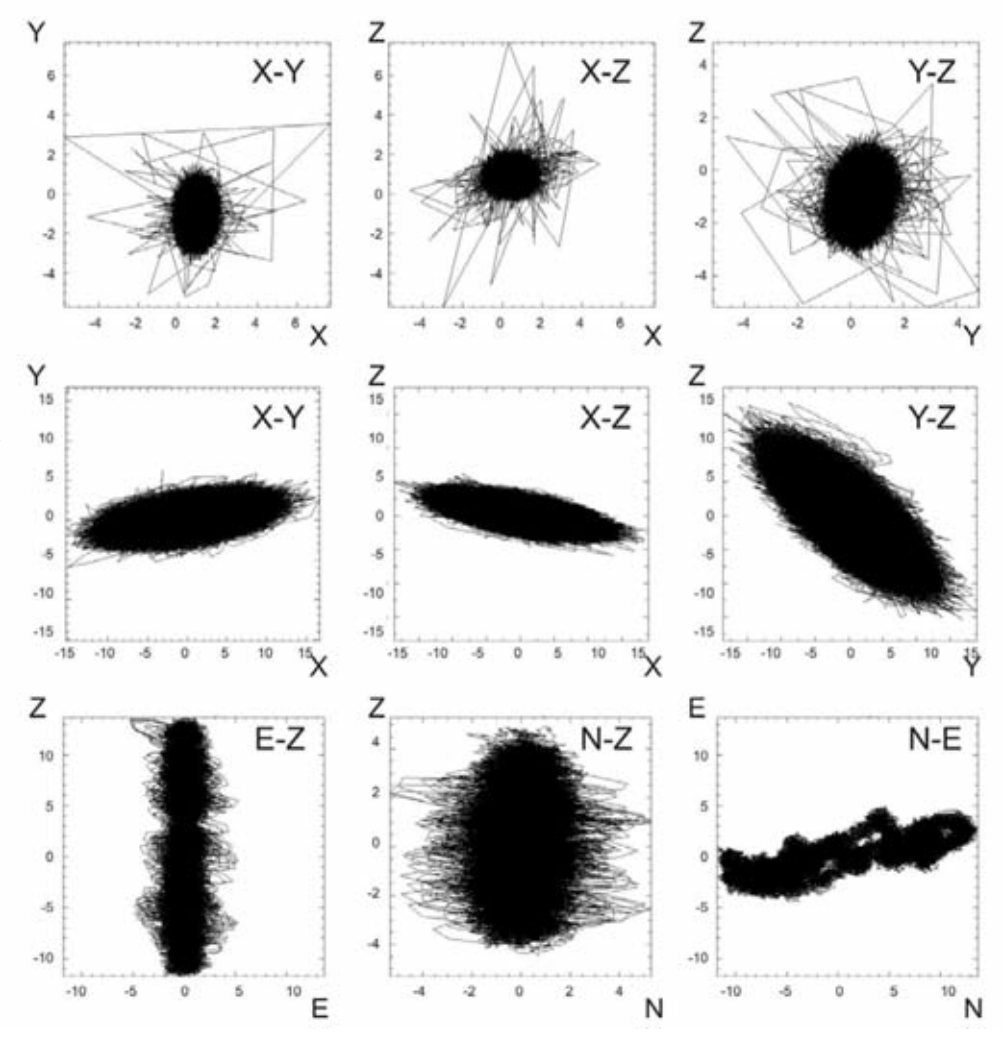

Fig. 5. Projections of the particle motion at the different sites: parking lot (upper row), Torrate test site (middle row) and Giant Cave (lower row).

The duration of each record is 10 minutes, due to the available RAM memory in the recording stations (4 Mbyte). As we ignore the statistical properties of the microtremors at the Torrate test site, we compared the amplitude spectra for three different recording periods: 10 minutes, 1 hour and 1 day (Fig. 6). The spectra were smoothed as for Fig. 3. Differences are large above 6 Hz and modest below 2 Hz, but not negligible in the intermediate frequency band. This spectral instability is not limited to that specific day. Repeating similar analyses in other days, the results remain very similar.

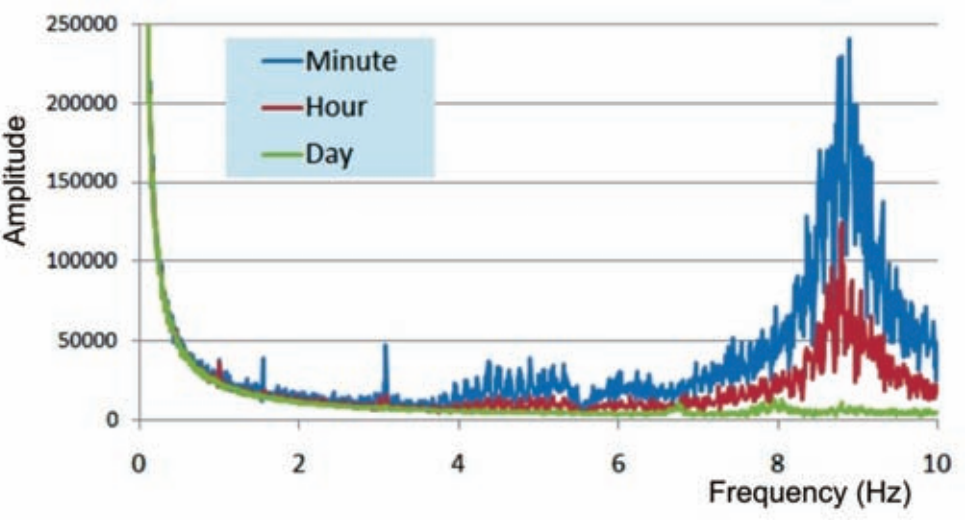

Fig. 6. Averaged amplitude spectra in the frequency range from 0 to 10 Hz, for a duration of 10 minutes (blue), 1 hour (red) and 1 day (green).

The spectral properties have been analyzed in detail in the literature, thus we preferred focusing further on the observed polarization and its stability. If microtremors are related to rock properties from deep formations (e.g., 1 km depth or more), not affected by daily or seasonal variations in the overburden, their propagation direction should be stable; it should also be nearly vertical, if the simple interpretation scheme adopted by van Maastrigt and Al-Dulaijan (2008) and Lambert et al. (2009) is appropriate.

STABILITY OF WAVE POLARIZATION

To study the stability of microtremor signals, we recorded the environmental noise continuously for 25 days using the 10-Hz three-component receiver at the Torrate test site. This area has been studied in detail for hydrological purposes by Giustiniani et al. (2008, 2009) and Picotti et al. (2009). The topography is flat and so are the interfaces of the rock formations, mainly fluvial deposits, for a depth exceeding 1 km. Fig. 7 shows a slice of the 3D depth-migrated volume of a high-resolution seismic survey in that area, and Fig. 8 is a cross-section calibrated by well logs. The water table is outcropping, and other aquifers are present at depths of about 50, 180, 280 and 470 m, respectively. In the surrounding region, the geophysical exploration did not find any evidence of hydrocarbons, so we do not expect spectral anomalies in the recorded signal.

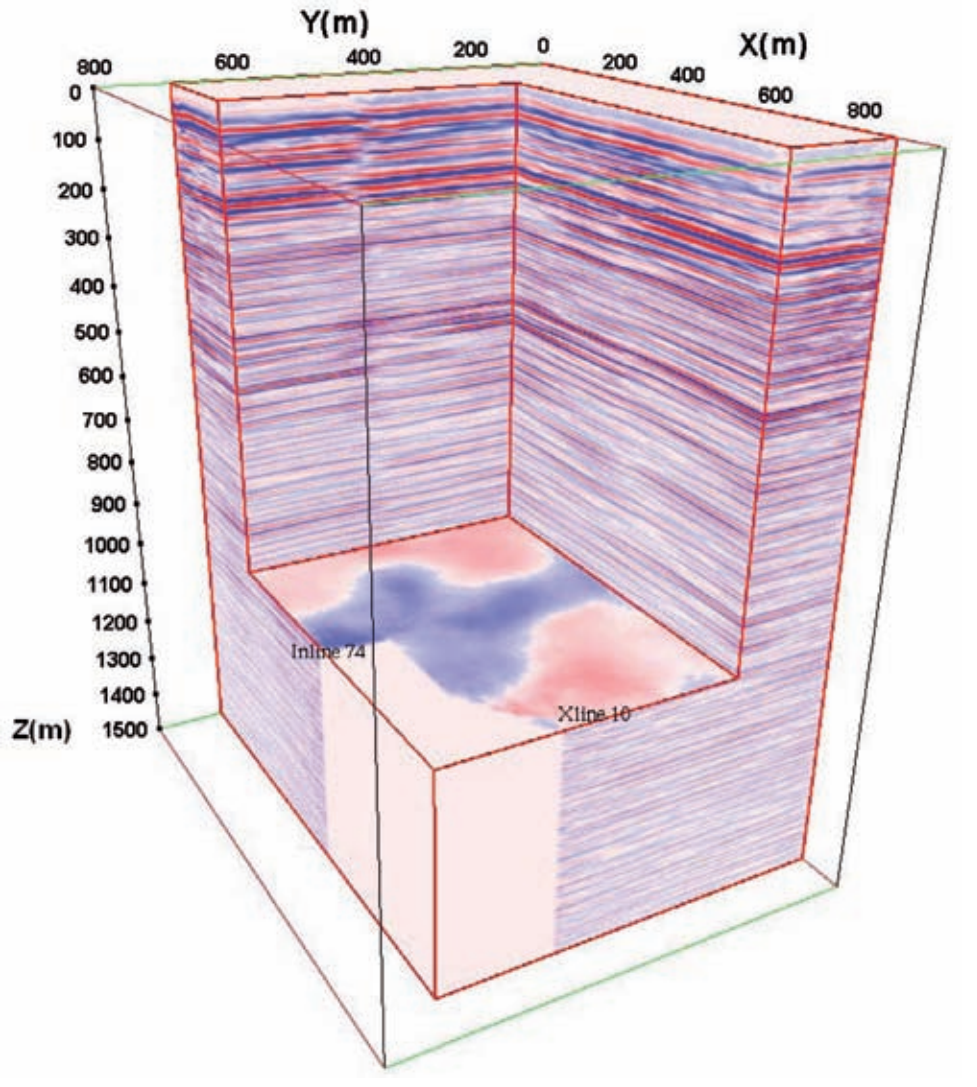

Fig. 7. Slice of the 3D depth-migrated volume of a high-resolution seismic survey in the Torrate area (modified from Picotti et al., 2009).

Although the area is relatively quiet, cars pass occasionally during the day on a local road nearby. Fig. 9 shows an uncorrelated Vibroseis record acquired in the area. We notice the hyperbolic noise from cars on the left, the Vibroseis signal (including both reflections and ground roll) at the centre and some linear noise due to far machinery, probably water pumps, on the right. Some noise-reduction techniques for passive seismic data have been presented by Lambert et al. (2010b).

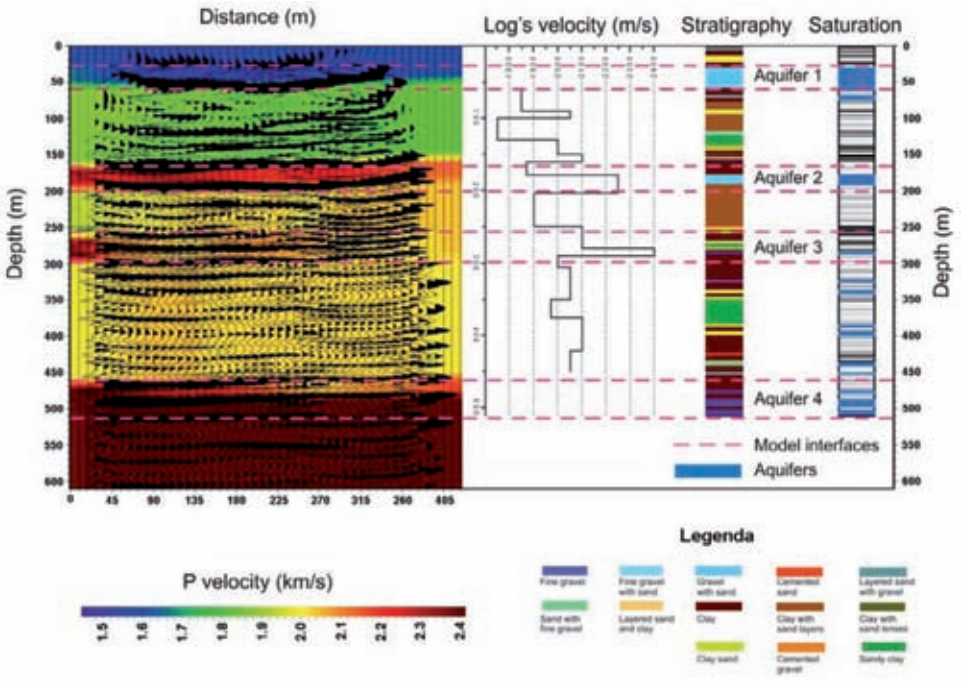

Fig. 8. A cross-section calibrated by well logs (modified from Picotti et al., 2009).

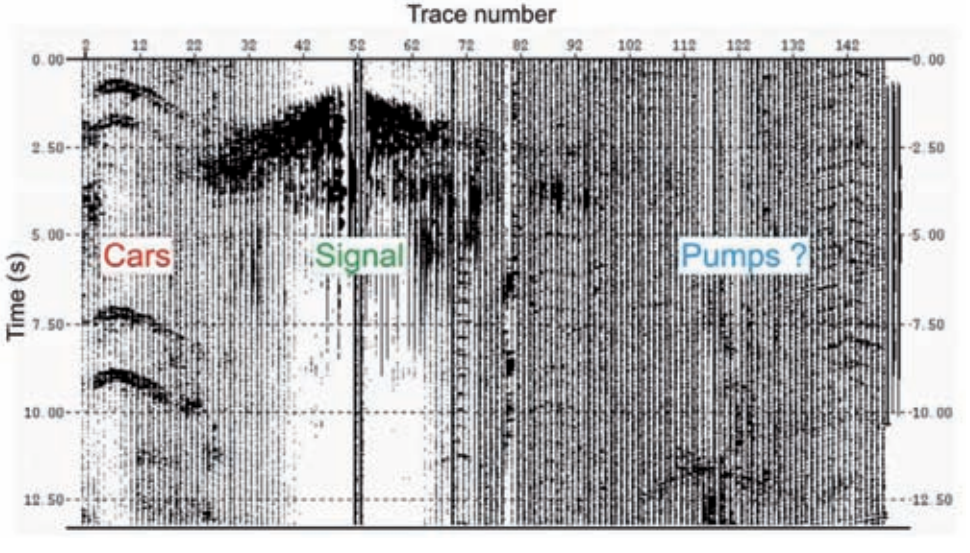

Fig. 9. Uncorrelated Vibroseis record, where we notice noise from cars (left), the seismic signal (centre) and a linear noise pattern (right), probably due to water pumps.

Fig. 10 displays the projections of the polarization angles in the three principal planes of a Cartesian reference system. As we expected a more quiet environment at night, the plot displays the average polarization for 25 consecutive days at midnight, for a time span of 10 minutes. The orientation of the plotted angles is explained in Fig. 11. We notice that all three projections change significantly from day to day. The purely azimuthal variation in the N-E plane evolves smoothly in time, but in a range between −10 and almost 20 degrees. The largest variations are those ones involving the vertical component. Such a component not only includes P-waves from teleseismic earthquakes, but also the vertical component of Rayleigh waves due to natural or human origin.

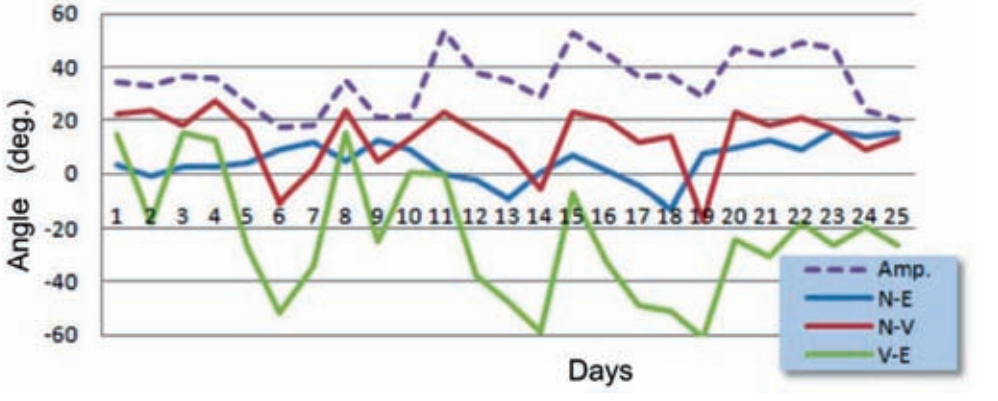

Fig. 10. Projections of the average polarization angles recorded for 25 consecutive days at midnight, with a duration of 10 minutes each.

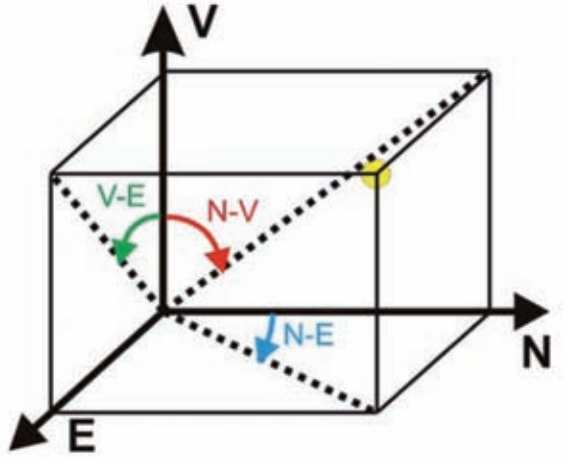

Fig. 11. The scheme explains the meaning of the projection angles in Figs. 10 and 12.

These surface waves are normally dominating, but also variable due to weather conditions and human work in progress. When surface waves are weaker, due to a quiet surface environment, the P-waves dominate instead with a different origin and propagation direction. Further measurements are needed to validate such a possible explanation.

When looking at variations during a single day (Fig. 12), the oscillations are even larger, although the azimuthal component remains the most stable. We notice in both time scales (Figs. 10 and 12) that there is a continuous curve in time, i.e., not a random noise pattern. Thus, the microtremor field evolves smoothly but continuously in time, although the causes for such a change need further investigations. We notice in Fig. 10 a correlation between the average

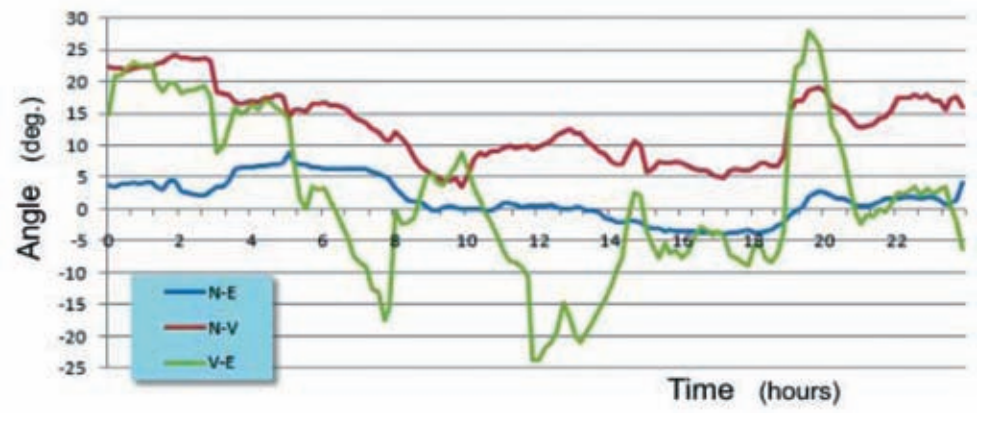

Fig. 12. Projections of the average polarization angles for a continuous recording during a full day, at time intervals of 10 minutes.

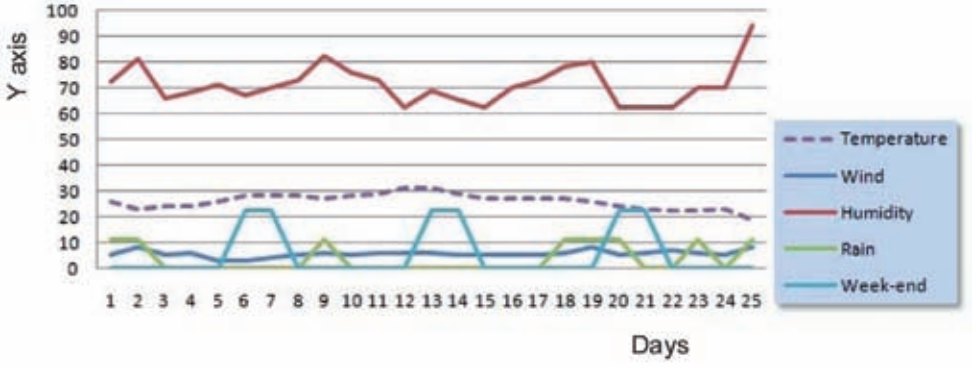

Fig. 13. Daily average values of a few possible influencing factors during the same period of microtremor data acquisition: temperature, wind speed, humidity, rain and calendar day type.

Fig. 14. Average azimuthal polarization direction (yellow line), between the minimum and maximum oscillation limits (red lines) observed during the 25-day survey, superimposed to the map of the Northern Adriatic Sea.

amplitude curve (dashed violet line) and the angles related to the dip component (red and green line), while it is minimal for the azimuthal component (blue curve). This correlation might be explained as mentioned above: strong surface waves show up and disappear, dominating or not a weaker background composed of teleseismic earthquakes with a different propagation path.

Fig. 13 shows a few possible elements to be considered, i.e., meteorological data as average pressure, temperature and wind speed in the same days as those ones in Fig. 10. Also, we highlighted the week-ends, when vehicle traffic and industrial machineries might have a different contribution. We do not notice any clear correlation of these elements with the polarization plot; probably a complex combination of them is affecting the signals. Further dedicated studies are needed for a better understanding of these phenomena. However, the average polarization direction during the 25 observation days is pointing towards the Adriatic Sea (Fig. 14). Quite intriguingly, such a direction is similar to that one observed by Ruigrok et al. (2011a, b) while analyzing the

polarization of background noise in Egypt. These directions are aligned along the Red Sea, i.e., an opening ocean ridge. These coincidences may be incidental, but might deserve further attention.

The average dip angle is about 26 degrees (Fig. 15). Such an angle could be explained by at least two types of impinging waves: either shallow head waves, whose steep final ray segment is consistent with the measured velocity field (Fig. 8); or by plane body waves from a source at some depth. This second option could relate microtremors to the properties of deep formations; however, in our case, the supposed rock anomalies could not be located vertically below the receivers, as suggested by van Maastrigt and Al-Dulaijan (2008). A good knowledge of the 3D velocity of P- and S-waves is needed to back-propagate the full wavefield to the possible deep origin of the microtremors, if any (Witten and Artman, 2011). Even assuming a simple, quasi-linear propagation path for the microtremors, the azimuth and dip of such a direction should be measured experimentally, but this is not found in the literature.

Rayleigh waves cannot contribute significantly to the average dip angle, as the horizontal layering implies vertical and horizontal axes for their elliptical particle motion. From a kinematic point of view, the vertical axis exceeds the minor one by a factor ranging from 1.2 to 1.9 at the earth's surface, depending on the Poisson ratio of the near-surface rocks (Landau and Lishitz, 1987). Therefore, we can expect an average vertical contribution from Rayleigh waves, but not the additional horizontal component observed in our experiments.

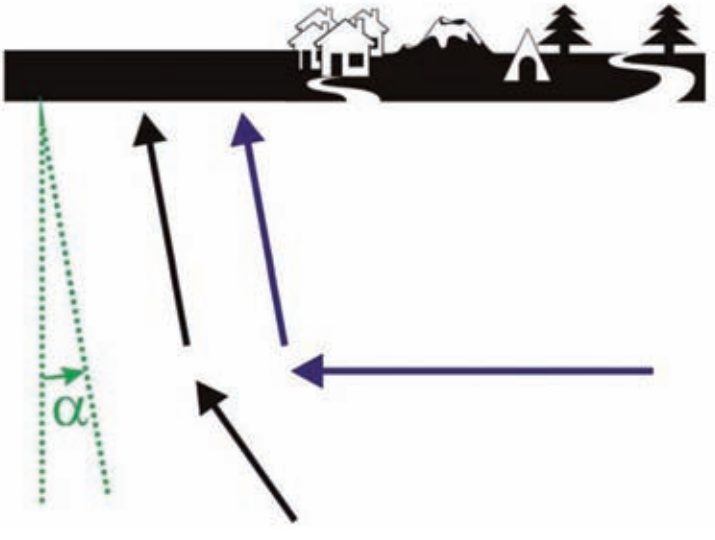

Fig. 15. Ambiguity of the interpretation of the polarization only: it can be explained, for example, both by shallow head waves and by direct arrivals from a source of arbitrary depth. The observed average dip angle α is about 26 degrees.

CONCLUSIONS

Our experiment shows that low-frequency microtremors are complex phenomena that change smoothly but quite rapidly in time. As the polarization depends both on the wave type and their propagation direction, its variability implies that it is affected at any moment by different causes and origin points. For this reason, it cannot be used immediately as a reliable indicator of possible underlying hydrocarbon reservoirs. Our experience is consistent with that of Ali et al. (2010), i.e., the dominant polarization direction is pointing towards the coast, suggesting the ocean waves as the main source of the microtremors. The removal of this effect and anthropogenic noise is being addressed by Riahi et al. (2011), among others, but is still an open challenge. Grevemeyer et al. (2000), Koper and de Foy (2008) and Koper et al. (2009) proved that strong seasonal effects exist too, so requiring their measurement and removal. Without such a further processing, the data is day-dependent, i.e., inconsistent with similar data acquired at some other date, even when using the same receiver at the same location.

A relevant spectral feature of the recorded background noise is its "pink colour", i.e., an amplitude function inversely proportional to the frequency. We showed that this cannot be due to electronic noise in the recording system, and remarked that such a trend has often been reported in the literature for weather, ocean phenomena and global seismicity. All these factors contribute to the background noise, so it is not surprising that the spectral features of the input are reproduced in some way in the output.

The presented experiment allows us to exclude the straightforward use of microtremors as possible direct hydrocarbon indicators in this area, because of the clear instability of this type of measurement. Similar results have been reported by Vesnaver et al. (2011) in a different area, overlying a major hydrocarbon reservoir. However, we cannot exclude it yet in general, as only well measurements may resolve ambiguities as presented in Fig. 15. Hodogram analysis is an important but not sufficient tool to assess the wave types that are being recorded.

The conclusions of this study cannot be extrapolated to other regions in a straightforward way. However, the cultural noise level, the geological setting and the relative vicinity to coasts are quite similar in large areas of Europe and other parts of the world. Our results do not exclude the general possibility to observe phenomena like that claimed by Lambert et al. (2009a), but the practical technology they presented. The latter one is weak and based on signals that are not stable. New recording or processing technology may be developed in the future, in the same way as for ground roll removal for standard active seismic surveys on land. If so, further attention will be deserved for these phenomena.

In principle, background noise, if not obscured by surface waves, can be used for imaging purposes provided that an accurate 3D velocity model in depth is available (Draganov et al., 2007, 2009; Steiner et al., 2008). Such an accurate model can only be obtained by active surface seismic surveys, possibly calibrated by a few wells.

ACKNOWLEDGEMENTS

The authors acknowledge the support of the King Fahd University of Petroleum and Minerals (KFUPM) and the Italian National Institute of Oceanography and Applied Geophysics (OGS). They thank in particular Elio Poggiagliolmi (Entec) for the detailed noise analysis in the Appendix. They also thank Alessandro Conighi, Stefano Picotti (OGS) and Gabor Korvin and Adnan Mubarak (KFUPM) for their technical contributions, and Peter Pecholcs (Saudi Aramco) and José Carcione (OGS) for fruitful discussions. Our work was partially supported by KFUPM in the Fast Track Program (Grant n. SB101007) and in the Deanship of Scientific Research Program (Grant n. RCRG101004). The SAC software was used for part of data processing (Goldstein and Snoke 2005).

REFERENCES

Aki, K. and Richards, P., 1980. Quantitative Seismology, Theory and methods. Freeman & Co., San Francisco.

Ali, M.Y., Berteussen, K.A., Small, J. and Barkat, B., 2010. Low-frequency passive seismic experiments in Abu Dhabi, United Arab Emirates: implications for hydrocarbon detection. Geophys. Prosp., 58: 875-899.

Berteussen, K.A., Ali, M.Y.A. and Small, J.S., 2008. A low frequency, passive experiment over a carbonate reservoir in Abu Dhabi - Wavefront and particle motion study. Extended Abstr., 70th EAGE Conf., Rome: B-046.

Bonnefoy-Claudet, S., Cotton, F. and Bard, P., 2006. The nature of noise wavefield and its applications for site effects studies: a literature review. Earth Sc. Rev., 79: 205-227.

Broadhead, M.K., 2010. Oscillating oil drops, resonant frequencies, and low-frequency passive seismology. Geophysics, 75: O1-O8.

Davidsen, J. and Schuster, H.G., 2002. Simple model for 1/f(α) noise. Phys. Rev., E 65: 026120.

Draganov, D., Wapenaar, C.P.A., Mulder, W., Singer, J. and Verdel, A., 2007. Retrieval of reflections from seismic background-noise measurements. Geophys. Res. Lett., 34: L04305.

Draganov, D., Campman, X., Thorbecke, J., Verdel, A. and Wapenaar, C.P.A., 2009. Reflection images from ambient seismic noise. Geophysics, 74: A63-A67.

Fraedrich, K. and Blender, R., 2003. Scaling of atmosphere and ocean temperature correlations in observations and climate models. Phys. Rev. Lett., 90: 108501.

Fraedrich, K., Luksch, U. and Blender, R., 2004. 1/f-model for long time memory of the ocean surface temperature. Phys. Rev. E, 70: 037301.

Frehner, M., Schmalholz, S.M. and Podladcikov, Y., 2009. Spectral modifications of seismic waves propagating through solids exhibiting a resonance frequency: a 1D coupled wave propagation-oscillation model. Geophys. J. Internat., 176: 589-600.

Gerstoft, P., Fehler, M.C. and Sabra, K.G., 2006. When Katrina hit California. Geophys. Res. Lett., 33: L17308.

Giustiniani, M., Accaino, F., Picotti, S. and Tinivella, U., 2008. Characterization of the shallow aquifers by high-resolution seismic data. Geophys. Prosp., 56: 655-666.

Giustiniani, M., Accaino, F., Picotti, S. and Tinivella, U., 2009. 3D seismic data for shallow aquifers characterization. J. Appl. Geophys., 68: 394-403.

Goldstein, P. and Snoke, A., 2005. Sac Availability for the IRIS Community. Incorporated Institutions for Seismology Data Management Centre. http://www.iris.edu/news/newsletter/vol7no1/page1.htm

Green, A. and Greenhalgh, S., 2009. Microtremor spectra: a proven means for estimating resonant frequencies and S-wave velocities of shallow soils/sediments, but a questionable tool for locating hydrocarbon reservoirs. First Break, 27: 43-50.

Green, A. and Greenhalgh, S., 2010. Comment on "Low-frequency microtremor anomalies at an oil and gas field in Voitsdorf, Austria" by Marc-André Lambert, Stefan Schmalholz, Erik H. Saenger and Brian Steiner, Geophys. Prosp., 57: 393-411. Geophys. Prosp., 58: 335-339.

Grevemeyer, I., Herber, R. and Essen, H. 2000. Micro-seismological evidence for a wave climate change in the northeast Atlantic Ocean. Nature, 408: 349-352.

Hanssen, P. and Bussat, S., 2008. Pitfalls in the analysis of low-frequency passive seismic data. First Break, 26: 111-119.

Holliger, K., 1996. Fault scaling and 1/f noise scaling of seismic velocity fluctuations in the upper crystalline crust. Geology, 24: 1103-1106.

Holzner, R., Eschle, P., Frehner, M., Saenger, E.H. and Steiner, B., 2009. Interpretation of hydrocarbon microtremors as nonlinear oscillations driven by oceanic background waves. Expanded Abstr., 79th Ann. Internat. SEG Mtg., Houston: 2294-2298.

Koper, K. and de Foy, B., 2008. Seasonal anisotropy in the short-period seismic noise recorded in South Asia. Bull. Seismol. Soc. Am., 98: 3033-3045.

Koper, K., de Foy, B. and Benz, H., 2009. Composition and variation of noise recorded at the yellow-knife seismic array. J. Geophys. Res., 114: B10310.

Lambert, M.A., Schmalholz, S.M., Saenger, E.H. and Steiner, B., 2009a. Low-frequency microtremor anomalies at an oil and gas field in Voitsdorf, Austria. Geophys. Prosp., 57: 393-411.

Lambert, M.A., Schmalholz, S.M., Saenger, E.H. and Steiner, B., 2009b. Passive seismic study at an oil and gas field in Voitsdorf, Austria. Extended Abstr., EAGE Workshop on Passive Seismic, Limassol (Cyprus): A34.

Lambert, M.A., Schmalholz, S.M., Saenger, E.H. and Steiner, B., 2010a. Reply to comment on "Low-frequency microtremor anomalies at an oil and gas field in Voitsdorf, Austria" by Marc-André Lambert, Stefan Schmalholz, Erik H. Saenger and Brian Steiner, Geophys. Prosp., 57: 393-411. Geophys. Prosp., 58: 341-346.

Lambert, M.A., Nguyen, T., Saenger, E.H. and Schmalholz, S.M., 2010b. Spectral analysis of ambient ground motion - Noise reduction techniques and a methodology for mapping horizontal inhomogeneity. J. Appl. Geophys., 58: 341-346.

Landau, L. and Lishitz, E., 1987. Theory of Elasticity, 3rd Ed. Butterworth-Heinemann, New York.

Lermo, J. and Chavez-Garcia, F.J., 1993. Site effect evaluation using spectral ratios with only one station. Bull. Seismol. Soc. Am., 83: 1574-1594.

Mandelbrot, B.B. and Wallis, J.R., 1969. Some long-run properties of geophysical records. Water Resour. Res., 5: 321-340.

Miller, G.F. and Pursey, H., 1955. On the partition of energy between elastic waves in a semi-infinite solid. Proc. Roy. Soc. London. Series A, Mathemat. Phys. Scien., 233: 55-69.

Nakamura, Y., 1989. A method for dynamic characteristics estimation of subsurface using microtremor on the ground surface. Quart. Rep. Railway Techn. Res. Inst., 30: 25-33.

Okada, H., 2003. The Microtremor Survey Method. Geophysical Monograph Series, 12. SEG, Tulsa, 135 pp.

Picotti, S., Giustiniani, M., Accaino, F. and Tinivella, U., 2009. Depth modeling and imaging of the 4D seismic survey of the Basso Livenza area (NE Italy). Boll. Geofis. Teor. Applic., 50: 71-82.

Peterson, J., 1993. Observations and modeling of background seismic noise. USGS Open File Rep., 93-322: 1-95.

Riahi, N., Birkelo, B. and Saenger, E.H., 2011. A statistical strategy to analyzing passive seismic attributes. Extended Abstr., 73rd EAGE Conf., Vienna: P198.

Ruigrok, E.N., Campman, X. and Wapenaar, C.P.A., 2011a. Extraction of P-wave reflections from microseisms. Compt. Rendus Geoscien., 343: 512-525.

Ruigrok, E.N., Campman, X. and Wapenaar, C.P.A., 2011b. A deep seismic profile from noise records. Extended Abstr., EAGE Workshop on Passive Seismic, Athens: PAS16.

Saenger, E.H., Schmalholz, S.M., Lambert, M.A., Nguyen T.T., Torres, A., Metzger, S., Habiger, R., Müller, T., Rentsch, S. and Mendez-Hernàndez, E., 2009. A passive seismic survey over a gas field: analysis of low-frequency anomalies. Geophysics, 74: O29-O40.

Selvam, A.M. and Fadnavis, S., 1998. Signatures of a universal spectrum for atmospheric inter-annual variability in some disparate climatic regimes. Meteorol. Atmospher. Phys., 66: 87-112.

Steiner, B., Saenger, E. and Schmalholz, S., 2008. Time reverse modeling of low-frequency microtremors: application to hydrocarbon reservoir localization. Geophys. Res. Lett., 35: L03307.

Telesca, L., Cuomo, V. and Lapenna, V., 2002. 1/f? fluctuations of seismic sequences. Fluctuat. Noise Lett., 2: L357-L367.

van Maastrigt, P. and Al-Dulaijan, A., 2008. Seismic spectroscopy using amplified 3C geophones. Extended Abstr., 70th EAGE Conf., Rome: B-047.

Vesnaver, A., Menanno, G., Kaka, S.I. and Jervis, M., 2011. 3D polarization analysis of surface and borehole microseismic data. Expanded Abstr., 81st Ann. Internat. SEG Mtg., San Antonio: PSC P2.

Witten, B. and Artman, B., 2011. Signal-to-noise estimates of time-reverse images. Geophysics, 76: MA1-MA10.

Zhang, J., Gerstoft, P. and Shearer, P., 2009. High-frequency P-wave seismic noise driven by ocean winds. Geophys. Res. Lett., 36: L09302.

APPENDIX

The contribution of "pink" or "red" noise (or "1/f noise") to the recorded signal depends on the data acquisition system features. The acquisition system used here for the purpose of evaluating the expected signal and noise levels consists of a Mark Products L-4 seismometer and a front-end operational amplifier chip, ADA4075-2, manufactured by Analog Devices. We assume that the signal representing the minimum level of the peak ground displacement sensed by the seismometer casing is 10^{-9} m at a frequency of 1 Hz. We assume also that this minimum signal level exceeds by an order of magnitude that of the seismometer-generated noise, expressed as the motion of its inertial mass. The noise consists of only the Brownian and thermal noise generators, which produce a voltage across the seismometer electrical terminals. This voltage in turn is transformed by modeling into an equivalent motion of the inertial mass. A noise model of the seismometer incorporating all the aforementioned features is beyond the scope of this appendix. For further details on seismometer noise see, for example, Aki and Richards (1980).

The velocity v(t) corresponding to the ground displacement can be expressed as:

$$v(t) = A\omega\cos(\omega t) \quad , \tag{A-1}$$

where: $A = 10^{-9}$ m, is the peak amplitude of the ground displacement and $\omega = 2\pi f$. The peak velocity v_P is:

$$v_P = A2\pi f = 10^{-9} \cdot 6.28 \cdot 1 \text{ m/s} \quad . \tag{A-2}$$

According to the manufacturer data, at 1 Hz, for a damping ratio set to 0.6 and the coil resistance equal to 5500 Ω, the seismometer transduction α is 4 volt/in/s, corresponding to 157 volt/m/s. Therefore, the peak voltage V_P produced by the peak velocity v_P is:

$$V_P = \alpha v_P = 157 \cdot 10^{-9} \cdot 6.28 \cdot 1 = 986 \text{ nV} \quad . \tag{A-3}$$

The noise spectral density of the operational amplifier, given by the manufacturer and referred to its input, is 6 nV at 1 Hz, whereas the peak-to-peak noise level over a range between 0.1 Hz and 10 Hz, spanning the 1/f region, is 60 nV. Both values differ from the peak level of the signal by more than an order of magnitude. We may therefore conclude that the "pink" noise generated in the amplifier is negligible with respect to the recorded signal.

Fig. A-1 is an experimental confirmation of these estimates. Using the actual amplitudes, we can see that the level of the records from a 10-Hz receiver (green line) and a 4.5-Hz receiver (red line) is much higher than the instrumental noise (black line), obtained by short-circuiting the recording instruments input terminals.

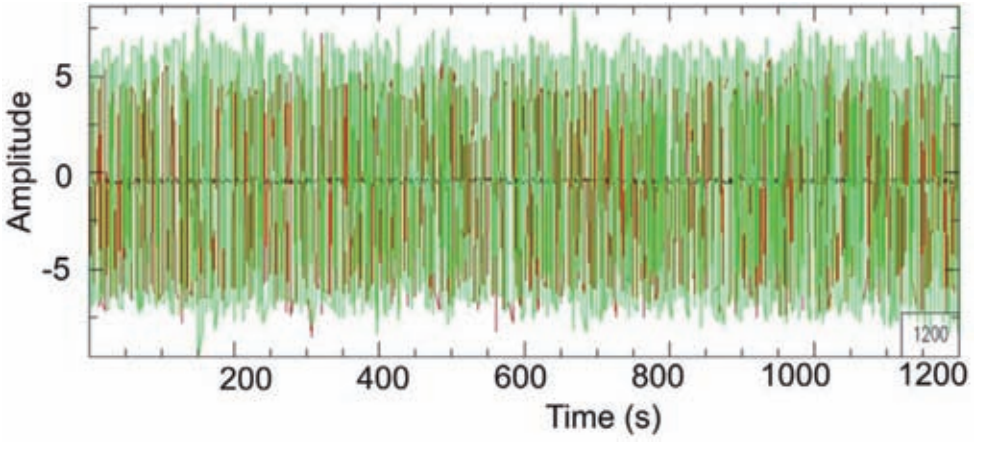

Fig. A-1. Amplitude comparison among records acquired with a receiver with peak frequencies of 10 Hz (green line), 4.5 Hz (red line) and without any receiver (black line).